Integrated Lane Change Model with Relaxation and Synchronization

Wouter J. Schakel, Victor L. Knoop, and Bart van Arem

A proposed lane change model can be integrated with a car-following model to form a complete microscopic driver model. The model resembles traffic better at a macroscopic level, especially regarding the amount of traffic volume per lane, the traffic speeds in different lanes, and the onset of congestion. In a new approach, lane change incentives are combined for determining a lane change desire. Included incentives are to follow a route, to gain speed, and to keep right. Classification of lane changes is based on behavior that depends on the level of lane change desire. Integration with a car-following model is achieved by influencing car-following behavior for relaxation and synchronization, that is, following vehicles in adjacent lanes. Other improvements of the model are trade-offs between lane change incentives and the use of anticipation speed for the speed gain incentive. Although all these effects are captured, the lane change model has only seven parameters. Loop detector data were used to validate and calibrate the model, and an accurate representation of lane distribution and the onset of congestion was shown.

Microscopic simulation is often used to evaluate the effects of traffic measures and new technologies. The strength of microscopic simulation is its high level of detail and accuracy. However, this generally comes at the expense of a high number of parameters, and calibration becomes a cumbersome and difficult process. Microscopic traffic models generally have two main components, a longitudinal (or car-following) model and a lateral (or lane change) model. In some cases the lane change model uses the car-following model, and this constitutes an integrated model.

Research has resulted in many car-following models, such as those of Gipps (*1*) and Wiedemann (*2*), the optimal velocity model (*3*), Tampère's model (*4*), and the intelligent driver model (IDM) (*5*). Lane change models, especially the aspect of mandatory lane changes, have received less attention. For instance, Kesting et al. (*6*) and Laval and Daganzo (*7*) look at speed only as an incentive to change lanes. Gipps was one of the first to formulate a model for lane changes that was intended to be integrated with a car-following model (*8*). Many lane change models since then have made a distinction between mandatory and discretionary lane changes. A problem with these models is that there is no trade-off between them. Toledo et al. recognized this and formulated a lane change model combined with incentives (*9*).

For most lane change models, it holds that gap acceptance either is a simple function of distance and speed difference or is based on a car-following model to determine resulting deceleration. The first class of gap-acceptance models fails to include car-following dynamics, whereas for the latter class it is assumed that drivers accept smaller gaps through a larger acceptable deceleration. However, in the real world, drivers largely will apply small decelerations and will accept smaller time headways for a while, as is shown empirically for merging traffic (*10*). This phenomenon is known as relaxation (*11–13*).

Another important aspect of lane changing is lane change preparation, sometimes referred to as the tactical stage (*6*), in which drivers may adapt their speed and align with a gap and in which another driver may create a gap. This lane change preparation is referred to as synchronization, as drivers synchronize with an adjacent lane. Little literature is available that describes models for synchronization and relaxation (*14–17*).

This brief overview of lane change models shows that there is a need for a new lane change model. The main goal is a good resemblance to the real world at the lane level regarding the amount of traffic on each lane (lane distribution) and the speed driven on each lane (lane speed). The model should be applicable for various road layouts and various levels of traffic density. For this goal to be met, multiple lane change incentives must be included. A secondary but still important goal is that the model resemble traffic dynamics, including the onset and progression of congestion. Relaxation and synchronization are included in the model to meet this goal. The final requirement is that it should be possible to calibrate the model, which requires that the complexity and number of parameters be limited. To the authors' knowledge, no lane change model fulfills these requirements.

This paper introduces a lane change model with relaxation and synchronization (LMRS), which includes both phenomena. Integration is discussed with a car-following model that uses an adapted version of the IDM (*5*). LMRS can be used with any car-following model that calculates vehicle acceleration. In this paper, some parameters are assumed to be part of the car-following model, but this is not a strict requirement. Integration with the car-following model is twofold. First, the car-following model is used for gap acceptance, where different headways apply because of relaxation. Second, synchronization triggers car following to vehicles in adjacent lanes as lane change preparation.

Most lane change models classify lane changes by the reason for which they are performed—mandatory, discretionary, courtesy, and so forth (*18*). Here, lane changes are classified by the way in which they are prepared and performed. This is called a lane change process, and different processes are performed for different levels of desire. In this paper, "desire" refers to lane change desire and "process" refers to the lane change process. Throughout, subscripts are dropped where possible for readability. Also, (t) for time-dependent quantities is dropped when possible; a reaction time is not included in the model.

Department of Transport and Planning, Faculty of Civil Engineering and Geosciences, Delft University of Technology, Stevinweg 1, P.O. Box 5048, 2600 GA Delft, Netherlands. Corresponding author: W. J. Schakel, w.j.schakel@tudelft.nl.

Transportation Research Record: Journal of the Transportation Research Board, No. 2316, Transportation Research Board of the National Academies, Washington, D.C., 2012, pp. 47–57.
DOI: 10.3141/2316-06

First, lane change desire and the accompanying processes are explained. Then the next section elaborates on the determination of lane change incentives. Integration with a car-following model is discussed next, followed by a section on calibration and validation.

LANE CHANGE DESIRE AND PROCESS

The main mechanism of LMRS, which is structured around lane change desire, is introduced in this section. The following symbols are used throughout the paper:

- $\dot{v}$ = acceleration as determined by car-following model;
- d = lane change desire;
- s = net distance headway;
- T = net time headway;
- k, i, j = specific, current, and target lane, respectively;
- v = speed;
- x = distance; and
- Δ = whether lane change is applicable (1) or not (0) for a specific incentive.

The desire to change from lane i to lane j that arises from the different incentives is combined into a single desire:

$$d^{ij} = d_r^{ij} + \theta_v^{ij} \cdot \left(d_s^{ij} + d_b^{ij}\right) \quad (1)$$

There is a desire to follow a route (d_r), to gain speed (d_s), and to keep right (d_b), where the subscript b stands for bias to a particular side. The latter two are included with θ_v which is the level at which voluntary (discretionary) incentives are included. The next section explains how these quantities are determined. Desire is meaningful between −1 and 1, where negative values indicate that a lane change is not desired (i.e., to stay or to change in the other direction). Values outside of the meaningful range may exist as incentives are added.

The total desire determines the behavior of drivers. Classification of lane changes is based on this behavior. Free lane changes (d_{free}), synchronized lane changes (d_{sync}), and cooperative lane changes (d_{coop}) are distinguished. Three thresholds relating to the processes are used to split the desire range into four subranges:

$$0 < d_{free} < d_{sync} < d_{coop} < 1 \quad (2)$$

Desire as calculated with Equation 1 falls within a particular range with an accompanying process. Figure 1 gives an overview of the variation of lane change behavior between processes. For little desire, no lane change will be performed. For a somewhat larger desire, a free lane change is performed that requires no preparation. For synchronized lane changes and cooperative lane changes, a potential lane changer is willing to synchronize speed with the target lane. This is achieved by following a vehicle in that lane. Concurrently this will align the vehicle with a gap (if there is a gap); this is thus a simple gap-searching model. In cooperative lane changes, the potential follower also will start to create a gap by following the potential lane changer. This behavior is also called synchronization and may be triggered for several reasons, such as the use of a turn indicator or the lateral in-lane position. An important reason, however, is the synchronization of the potential lane changer itself. From this behavior a driver may deduce that an adjacent vehicle wants to change lanes. Throughout this paper, it is assumed that drivers can note whether the lane change desire of another driver is smaller or larger than d_{coop}. Empirical evidence that drivers are willing to create a gap, at least at an on-ramp, can be found in the work by Daamen et al., where no merging vehicle is overtaken by multiple vehicles (*10*).

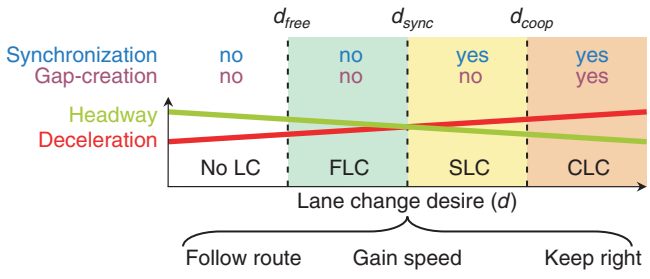

FIGURE 1 Overview of LMRS. Lane change desire is based on three incentives. Lane change behavior, including accepted headway and deceleration for lane change, varies depending on level of lane change desire.

In addition to synchronization, desire-dependant differences in the accepted headway and deceleration will arise if a lane change is initiated. For higher desire, drivers are willing to accept smaller headways and to decelerate more. However, the maximum deceleration will be smaller in the model presented here than in most existing lane change models, such as MOBIL (*6*), in which a value of 4 m/s^2, which is rather high, is used. This is achieved by allowing for relaxation and synchronization.

Desire to change both left and right is determined. Also the possibility (gap acceptance) to both sides is assessed. The lane change with highest desire will be performed if possible and desired ($d \geq d_{free}$). If the lane change is not possible, lane change preparation (synchronized and cooperative lane changes) may be performed.

LANE CHANGE INCENTIVES

This section elaborates on the quantities of Equation 1 in detail. In this paper, asymmetric traffic rules are assumed, by which drivers must keep right and may overtake only on the left. Consequently, a speed advantage is considered only for the left lane, and in certain circumstances there may be a bias to the right. In the model, vehicles are not explicitly prevented from overtaking on the right, because this often happens in the real world despite the prohibition. However, a speed advantage is not actively considered in the right lane. The model can be easily adapted for symmetric or left-hand traffic rules.

Several parameters are introduced in this and the next sections. Table 1 provides an overview of all parameters.

Anticipation Speed

The voluntary incentives described in the following subsections use anticipation speed. The following definitions are used to determine this quantity:

- v_{ant} = anticipation speed, or considered speed at lane;
- v_{lim} = speed limit;
- v_{max} = maximum vehicle speed;
- v_{des} = desired speed;
- v_{lead} = actual speed of (adjacent) leader;
- $\tilde{v}_{lead}$ = considered speed of (adjacent) leader given headway;
- x_0 = anticipation distance; and
- δ = speed limit adherence factor.

TABLE 1 Overview of Model Parameters

Symbol	Initial or Assumed Value	Calibration[a]	Calibrated Value	Remarks[b]
Regular Car-Following Parameters				
a_{truck}	0.4 m/s^2	Fixed		Taken from FOSIM (*19*).
a_{car}	1.0 m/s^2	Congestion	1.25 m/s^2	A value of 0.73 was found (*5*). This, however, pertains to mixed traffic. Cars start somewhat higher.
b	1.67 m/s^2	Congestion	2.09 m/s^2	A value of 1.67 was found (*5*), which was used here.
T_{max}	1.2 s	Congestion	1.2 s	On the left lane of the two-lane section of network, maintainable flows of around 2,400 veh/h were found. From this, a value of 1.2 s at 90 km/h was calculated.
s_0	3 m	Fixed		This value is based on the length of cars and a jam density of about 140 pce/km.
$v_{des,car}$	123.7 km/h	Free flow	123.7 km/h	A cumulative Gaussian distribution was fitted to the average speeds in free flow on the middle and left lanes using the fractions of traffic on these lanes. 5% was added to the resulting fit as this approach gives a lower limit to desired speed.
σ_{car}	8.3 km/h	Free flow	12.0 km/h	See $v_{des,car}$.
$v_{des,truck}$	85 km/h	Fixed		Taken from FOSIM (*19*).
σ_{truck}	2.5 km/h	Fixed		It is assumed that the majority of trucks has a desired speed of 80 to 90 km/h.
l_{car}	4 m	Fixed		Estimated using helicopter data from Hoogendoorn et al. (*20*).
l_{truck}	15 m	Fixed		Estimated using helicopter data from Hoogendoorn et al. (*20*).
Lane Change–Related Parameters				
T_{min}	0.7 s	Congestion	0.56 s	Average minimum headway of 0.7 s is assumed (*10*).
τ	20 s	Congestion	25 s	Some studies (*11–13*, *16*) estimate values between 20 and 30 s. Because of exponential relaxation a value at the lower end was assumed.
x_0	300 m	Free flow	295 m	Based on the last traffic signs indicating a lane drop.
t_0	67 s	Free flow	43 s	Value of 50 s resembles driver behavior (*8*). This is set equal to $t_0 \cdot (1 - d_{free})$, where lane changes start.
d_{free}	0.25	Free flow	0.365	Starts with four equal desire ranges.
d_{sync}	0.50	Related	0.577	The range beyond d_{free} is equally divided, $d_{sync} = d_{free} + \frac{1}{3}(1 - d_{free})$.
d_{coop}	0.75	Related	0.788	The range beyond d_{free} is equally divided, $d_{coop} = d_{free} + \frac{2}{3}(1 - d_{free})$.
v_{gain}	70 km/h	Free flow	69.6 km/h	Based on d_{free} and speed differences between lanes in the order of 15 to 20 km/h on road stretch, starts with 70 km/h.
v_{crit}	60 km/h	Fixed		Estimated on plots of speed vs. lane fraction where in the range around 60 km/h, fractions tend to become more equal.

NOTE: pce = passenger car equivalents.
[a]Whether value is fixed, related to another parameter, or calibrated in scenario.
[b]Describes how initial or assumed values have been determined. Values were additionally determined with few initial runs of model.

The anticipation speed is intended to represent to what extent drivers take account of downstream vehicles. The further away the vehicle is, the less influence the vehicle has. The slower a vehicle is, the more it may reduce the anticipation speed. The anticipation speed v_{ant} on a lane is a function of v_{lim}, v_{max}, and v_{lead}, where v_{lead} is considered for several leading vehicles (potentially) on the assessed lane. The quantities v_{lim} and v_{max} are combined into a desired speed for lane k as

$$v_{des}^{k} = \min\left(\delta \cdot v_{lim}^{k}, v_{max}\right) \tag{3}$$

This expression includes a level of adherence δ with regard to the speed limit. For $\delta > 1$, this results in speeding, and for $\delta < 1$ this results in the opposite.

The speed of any leading vehicle v_{lead} may influence the anticipation speed. A slow leader lowers the anticipation speed; however, if this leader is very far away, the vehicle is not considered at all. $\tilde{v}_{lead}(s = 0) = v_{lead}$ where the vehicle is fully considered and $\tilde{v}_{lead}(s = x_0) = v_{des}$ where the vehicle is completely ignored. The anticipation distance used is x_0, which is also a parameter for the route incentive as described in the next subsection. For intermediate headways linear interpolation gives

$$\tilde{v}_{lead} = \left(1 - \frac{s}{x_0}\right) \cdot v_{lead} + \frac{s}{x_0} \cdot v_{des} \tag{4}$$

The anticipated speed on lane k is given by

$$v_{ant}^{k} = \min\left(v_{des}^{k}, \min_{m \in M_k}\left(\tilde{v}_{lead}^{m}\right)\right) \tag{5}$$

where all leading vehicles from the set M_k are taken into account. This set is lane dependant and entails vehicles with a headway shorter than x_0. The set M_k by definition entails all vehicles on lane k, all vehicles on lane $k - 1$ (left) with $d^{k-1,k} \geq d_{coop}$, and all vehicles on lane $k + 1$ (right) with $d^{k+1,k} \geq d_{coop}$. Vehicles with $d^{k,j} \geq d_{coop}$ if $k = i$ (i being the current and j being the considered lane), however, are never considered. In other words, all vehicles on, or potentially on, a certain lane are considered for the anticipation speed on that lane. When the anticipation speed on an adjacent lane is assessed, potential lane changers from the current lane are excluded. This exclusion is put in place to prevent situations in which large speed differences between lanes are persistently maintained as drivers anticipate a slow speed on the faster lane because of other slow vehicles with a desire toward that lane.

Speed Incentive

It is assumed that drivers may desire to change lane to increase their speed. It is also assumed that drivers are particularly anticipative when assessing the speed on a lane, that is, if possible, flying takeovers are performed so that no speed is actually lost. Therefore, the anticipation speed is used to assess the desire. The following assumptions are made about the speed incentive:

- A full desire is experienced for a speed gain of v_{gain}.
- Desire is linearly related to speed gain.
- Drivers ignore a possible speed gain toward the right lane at high speeds ($v_{\text{ant}} > v_{\text{crit}}$).
- Desire to change lane is reduced during acceleration.

For the latter assumption, a_{gain} is introduced as a reduction factor on desire. It is defined as

$$a_{\text{gain}} = \frac{a - \max(\dot{v}, 0)}{a} \tag{6}$$

where a is the maximum acceleration from the car-following model. Also, Δ_s defines if a lane change is possible and allowed ($\Delta_s = 1$) or not ($\Delta_s = 0$). Desire from the speed incentive is now defined as

$$d_s^{i,i-1} = \begin{cases} a_{\text{gain}} = \dfrac{v_{\text{ant}}^{i-1} - v_{\text{ant}}^{i}}{v_{\text{gain}}} & \Delta_s^{i,i-1} = 1 \\ 0 & \Delta_s^{i,i-1} = 0 \end{cases}$$

$$d_s^{i,i+1} = \begin{cases} a_{\text{gain}} = \dfrac{\min\left(v_{\text{ant}}^{i+1} - v_{\text{ant}}^{i}, 0\right)}{v_{\text{gain}}} & \Delta_s^{i,i+1} = 1 \text{ and } v_{\text{ant}}^{i} > v_{\text{crit}} \\ a_{\text{gain}} \dfrac{v_{\text{ant}}^{i+1} - v_{\text{ant}}^{i}}{v_{\text{gain}}} & \Delta_s^{i,i+1} = 1 \text{ and } v_{\text{ant}}^{i} \le v_{\text{crit}} \\ 0 & \Delta_s^{i,i+1} = 0 \end{cases} \tag{7}$$

where $i - 1$ and $i + 1$ are the left and right adjacent lanes, respectively. Note that a speed loss is always considered toward the right lane to be balanced with other incentives.

Because the speed incentive is based on anticipation speed, it is also based on adjacent vehicles that have $d > d_{\text{coop}}$. If these vehicles lower the anticipation speed, a driver may be triggered to perform a courtesy lane change. These are lane changes that are performed to create a gap for another vehicle.

Route Incentive

If the current lane will not allow a route to be followed, desire for lane change arises. This may be because the lane ends or because the lane will change direction. The following assumptions are made for these situations:

- At relatively high speeds, the remaining time per required lane change determines desire. This is different from existing models such as that of Gipps (*8*) and the FOSIM lane change model (*19*), in which desire is based on distance. Desire starts at a remaining time of t_0 per lane change.
- At relatively low speeds, the remaining distance becomes dominant in determining desire. Desire starts at a remaining distance of x_0 per lane change.
- Desire increases linearly toward full desire for decreasing time or distance.
- Desire from the route incentive exists even if the lane change is (currently) not possible.

The latter assumption may trigger synchronization upstream of an actual merge location, which is common practice at merge locations. For determining desire for the route incentive, x_r^k is the remaining distance, $t_r^k = x_r^k / v$ is the remaining time given current speed v, and n_r^k is the number of required lane changes, all for lane k. Desire is now determined as

$$d_r^k = \max\left(1 - \frac{x_r^k}{n_r^k \cdot x_0}, 1 - \frac{t_r^k}{n_r^k \cdot t_0}, 0\right) \tag{8}$$

which defines the desire to leave lane k. For deriving the desire for either the left or the right lane, the desire on the target and that on the current lane are compared. If the desire to leave the target lane is smaller than the desire to leave the current lane, the desire to leave the current lane is used. Conversely, the negative value of the desire to leave the target lane is used, that is, the lane change is undesired with the amount to leave the target lane. This is defined as

$$d_r^{ij} = \begin{cases} d_r^i & \Delta_r^j = 1 \text{ and } d_r^i > d_r^j \\ 0 & \Delta_r^j = 1 \text{ and } d_r^i = d_r^j \\ -d_r^j & \Delta_r^j = 1 \text{ and } d_r^i < d_r^j \\ -\infty & \Delta_r^j = 0 \end{cases} \tag{9}$$

where $\Delta_r = 1$ indicates that the route can still be followed on the target lane.

Keep-Right Incentive

A simple incentive in accordance with the "keep right if possible" traffic rule that is implemented in many models is a constant bias to the right lane, such as in MOBIL (*6*). Drivers will be inclined to change to the right; however, the phrase "if possible" is stretched if drivers are forced to drive somewhat more slowly than their desired speed. The slugs and rabbits theory of Daganzo predicts more traffic on the left lane for typical percentages of slow traffic (*21*). However, if there is no slow traffic on the right lane for a considerable distance, a driver would at some point move to the right. Here, the lane change threshold d_{free} must be compensated only whenever a vehicle anticipates unhindered speed on the right lane.

Another influence on right-keeping behavior is a downstream turn. Drivers are not willing to move right if that lane will turn into a wrong direction, even in light traffic conditions. If a driver is within the region defined by t_0, it will experience a slight negative desire to change right. In that case it is assumed that drivers do not obey the traffic rule. In short, drivers will obey the keep-right rule only if the situation on the right lane is not worse for speed and route. This is expressed as

$$d_b^{i,i-1} = 0$$

$$d_b^{i,i+1} = \begin{cases} d_{\text{free}} & v_{\text{ant}}^{i+1} = v_{\text{des}} \text{ and } d_r^{i,i+1} \ge 0 \\ 0 & \text{otherwise} \end{cases} \tag{10}$$

Consideration of Incentives

Depending on the urgency of mandatory lane changes, drivers may (partially) ignore voluntary lane change incentives. Therefore θ_v is used, which is the level at which voluntary desire is included in the decision. It depends on the level of (negative) mandatory desire, which may become dominant. Total voluntary desire $d_v = d_s + d_b$ is used for an example. If both voluntary and mandatory desire are either negative or positive ($d_r \cdot d_v \geq 0$), voluntary desire is fully included because it coincides with mandatory desire. However, if voluntary desire conflicts with mandatory desire ($d_r \cdot d_v < 0$), the voluntary desire is only partially included. For strong mandatory desire, negative or positive ($|d_r| > d_{\text{coop}}$), voluntary desire is ignored. For mild mandatory desire ($|d_r| < d_{\text{sync}}$), voluntary desire is fully included. In between, the consideration of voluntary desire is linearly interpolated. This is expressed as

$$\theta_v^{ij} = \begin{cases} 0 & d_r^{ij} \cdot d_v^{ij} < 0 \text{ and } \left|d_r^{ij}\right| \geq d_{\text{coop}} \\ \dfrac{d_{\text{coop}} - \left|d_r^{ij}\right|}{d_{\text{coop}} - d_{\text{sync}}} & d_r^{ij} \cdot d_v^{ij} < 0 \text{ and } d_{\text{sync}} < \left|d_r^{ij}\right| < d_{\text{coop}} \\ 1 & \underbrace{d_r^{ij} \cdot d_v^{ij} \geq 0}_{\text{conflict/coincide}} \text{ or } \underbrace{\left|d_r^{ij}\right| \leq d_{\text{sync}}}_{\text{mandatory dominance}} \end{cases} \tag{11}$$

INTEGRATION WITH A CAR-FOLLOWING MODEL

How the lane change model determines the desire to change lane has been discussed. This section addresses integration with a car-following model related to gap acceptance and relaxation and gap creation and synchronization.

Gap Acceptance and Relaxation

A gap is accepted or rejected on the basis of the resulting deceleration that follows from the car-following model. Gaps that result in deceleration that is too large are rejected because they are unsafe, uncomfortable, or impolite. This is similar to MOBIL (*6*), except that the applicable headway is changed. The gap is accepted if both the lane changer (c) and the new follower (f) will have an acceleration that is larger than some safe deceleration threshold $-b^c$ as in

$$\dot{v}^g \geq -b^c \cdot d^{ij,c} \tag{12}$$

with $g \in \{c,f\}$. For clarity, to which vehicle the parameters pertain is explicitly given. The applicable headway for both the lane changer and the new follower is given by

$$T^g\left(d^{ij,c}\right) = \min\left(T^g\left(t\right), \left\langle d^{ij,c}\right\rangle \cdot T^g_{\min} + \left(1 - \left\langle d^{ij,c}\right\rangle\right) \cdot T^g_{\max}\right) \tag{13}$$

where

$T^g(t)$ = current following time headway of vehicle g including previous relaxation,
$T^g_{\max}$ = regular following time headway of vehicle g,
$T^g_{\min}$ = minimum following time headway at maximum desire of vehicle g, and
$\langle d^{ij,c}\rangle$ = lane change desire of vehicle c limited between 0 and 1.

Equations 12 and 13 show that for larger desire, larger decelerations and shorter headways are accepted. If the lane change is initiated, both vehicle c and vehicle f should update the value for $T^g(t)$ to the value of $T^g(d^{ij,c})$. The relaxation of the headway value is assumed exponential with relaxation time τ. In a numerical update scheme with time step Δt one can use

$$T\left(t\right) = T\left(t - \Delta t\right) + \left\{T_{\max} - T\left(t - \Delta t\right)\right\}\frac{\Delta t}{\tau} \tag{14}$$

Synchronization and Gap Creation

When lane change desire is above the synchronization threshold, drivers will start to synchronize their speeds with the leader on the target lane by applying the car-following model resulting in $\dot{v}^{ij}_{\text{sync}}$. Drivers will apply a maximum deceleration of b, which is considered both a comfortable and a safe deceleration. The maximum deceleration for speed synchronization is given by

$$\dot{v}^{ij}_{\text{sync}} > -b \tag{15}$$

If an adjacent leader wishes to change lanes with a desire above the cooperation threshold, a gap will be created. Gap creation is very similar to synchronization, and the car-following model is again applied with a limited deceleration, as in Equation 15.

Car-Following Model

A slightly adapted version of the IDM by Treiber et al. is used (*5*). The acceleration is calculated with

$$\dot{v} = a \cdot \min\left(1 - \left(\frac{v}{v_{\text{des}}}\right)^4, 1 - \left(\frac{s^*}{s}\right)^2\right) \tag{16}$$

and

$$s^* = s_0 + v \cdot T + \frac{v \cdot \Delta v}{2\sqrt{a \cdot b}} \tag{17}$$

where

s_0 = stopping distance,
Δv = approaching rate to leader,
s = net distance headway, and
s^* = dynamic desired headway.

The adapted model is referred to as IDM+ and differs from the IDM in the minimization over, instead of addition of, components in Equation 16. This adaptation has been made to increase the capacity to more realistic values, as well as to have $\dot{v} = 0$ for $v = v_{\text{des}}$ and $s = s^*$. Details are available elsewhere (*22*).

Car-following models are usually designed for in-lane dynamics. In multilane traffic, headways and speed difference between lanes have a wider range of values. In the IDM, negative values of either s or s^* have the same effect as positive values because of the power of two. Negative headways occur for adjacent vehicles, and a negative dynamic desired headway may occur for large negative values of Δv. Therefore, the following boundary conditions are used:

$$\begin{aligned} s &> 0 \\ s^* &\geq 0 \end{aligned} \tag{18}$$

CALIBRATION AND VALIDATION

This section describes the model calibration and validation. Model implementation, calibration setup, and data are discussed, and the results are given.

Model Implementation

Although the LMRS has been presented in detail, the precise implementation can influence model results. This section presents the implementation. The following procedure should be performed for each driver at each time step. The minimum acceleration based on all applicable leaders should be used. A lane change duration of 3 s was used (*19*), during which a virtual and temporary vehicle was placed on the target lane to prevent other lane changes toward the same location. On the first 100 m of the network, lane changes are never performed because upstream vehicles that influence such a lane change may not yet be generated. $\Delta t = 0.5$ s (from FOSIM) was used as a balance between short running times and modeling precision (*19*). On a dual CPU with 2.8 GHz, this results in running times on the order of 10 50 s per modeled hour, depending on the level of congestion (i.e., number of vehicles ranging from 150 to 600). The steps and relevant equations are as follows:

- While not changing lane,
  - Relax headway (Equation 14),
  - Calculate route desire (Equations 8 and 9),
  - Calculate anticipated speeds (Equations 3 through 5),
  - Calculate speed desire (Equations 6 and 7),
  - Calculate keep-right desire (Equation 10),
  - Combine desires (Equations 11 and 1),
  - Gap-acceptance (Equations 12 and 13),
  - Make lane change decision,
  - Follow leader (Equations 16 through 18),
  - If applicable, synchronize (Equations 16 through 18, Equation 15), and
  - If applicable, create gap (Equations 16 through 18, Equation 15) and
- During lane change, follow old and new leader (Equations 16 through 18).

Calibration Setup

The LMRS is applied in combination with the IDM+. The full model has 20 parameters, which are too many to calibrate—calculation would take a long time, and a solution would be difficult to find because there are many degrees of freedom. This problem is alleviated in two ways. Not all parameters are calibrated because some are well known. Two parameters, d_{sync} and d_{coop}, are related to d_{free}, reducing from nine to seven the number of parameters pertaining to lane changes. Second, two calibration scenarios are used. In the first scenario, the model is calibrated to free-flow conditions, calibrating parameters that can be determined in free flow. In the second scenario, the model is calibrated to congested conditions, calibrating the remaining parameters. This approach follows the reasoning of Ossen and Hoogendoorn (*23*). The benefits of this approach are that each iteration of the calibration procedure involves fewer model runs, the calibration will converge in fewer iterations, and the free-flow runs are of short duration.

Table 1 gives an overview of all model parameters. Two classes, passenger cars and trucks, are applied. Parameters are equal between classes except acceleration (a), vehicle length (l), and desired speed. For cars, it is assumed that the desired speed is given by driver preference $\delta_{car} = N(v_{des,car}, \sigma_{car})/v_{lim}$, where $N(v_{des,car}, \sigma_{car})$ is a Gaussian distribution with mean $v_{des,car}$ and standard deviation σ_{car}. For trucks, it is assumed that the desired speed is given by the maximum vehicle speed $v_{max,truck} = N(v_{des,truck}, \sigma_{truck})$.

Two calibration scenarios are used. Parameter values found in the free-flow scenario, which is performed first, are used in the congestion scenario. The error measure ε, which should be minimized, is based on a comparison of real and virtual detector data. In free flow, the following is used:

$$\varepsilon_{free} = \sqrt{\frac{\sum_{n=1}^{N}\left(\left(\sum_{t=1}^{H} q_{n,t}^{real} - \sum_{t=1}^{H} q_{n,t}^{sim}\right)^2\right)}{N}} + 25 \cdot \sqrt{\frac{\sum_{n=1}^{N}\left(\left(\frac{H}{\sum_{t=1}^{H}\frac{1}{v_{n,t}^{real}}} - \frac{H}{\sum_{t=1}^{H}\frac{1}{v_{n,t}^{sim}}}\right)^2\right)}{N}} + m \quad (19)$$

where

$t = 1, \ldots, H$ = considered time period,
$n = 1, \ldots, N$ = considered detectors,
q = 1-min flow count,
v = arithmetic mean speed of all vehicles within 1 min, and
m = number of deleted vehicles in simulation.

The first part of Equation 19 is the root mean square error (RMSE) of hourly flow ($H = 60$) of all detectors. The second part of Equation 19 is the RMSE of the harmonic mean of speed measurements. The RMSE relating to speed with a factor of 25 is included, meaning that an error of 25 vehicles per hour is equal to an error of 1 km/h. Finally the number of deleted vehicles is included because, depending on the parameter values, drivers in the model may not be able to change lanes before they have to. This is included to keep the number of deleted vehicles small.

The following is used for the congestion scenario:

$$\varepsilon_{cong} = \sqrt{\frac{\sum_{n=1}^{N}\sum_{t=1}^{H}\left(60 \cdot \left(q_{n,t}^{real} - q_{n,t}^{sim}\right)\right)^2}{N \cdot H}} + 25 \cdot \sqrt{\frac{\sum_{n=1}^{N}\sum_{t=1}^{H}\left(v_{n,t}^{real} - v_{n,t}^{sim}\right)^2}{N \cdot H}} + m \quad (20)$$

which is similar to Equation 19. Minute measurements, however, are not aggregated in order to capture the dynamics of congestion. For an equal comparison between flow and speed, the minute flows are calculated to hourly flows.

A calibration algorithm is used to find the optimal parameter values. It starts with a large search space, which is incrementally reduced in the second step. As soon as the search space is smaller than 0.1% of the parameter values, the algorithm stops. This method is unable to change the sign of a parameter, which is not a problem for the parameters here. The optimization algorithm is as follows:

0. Start with x as the initial value of the parameters. Set $f = \{0.8, 1.25\}$.

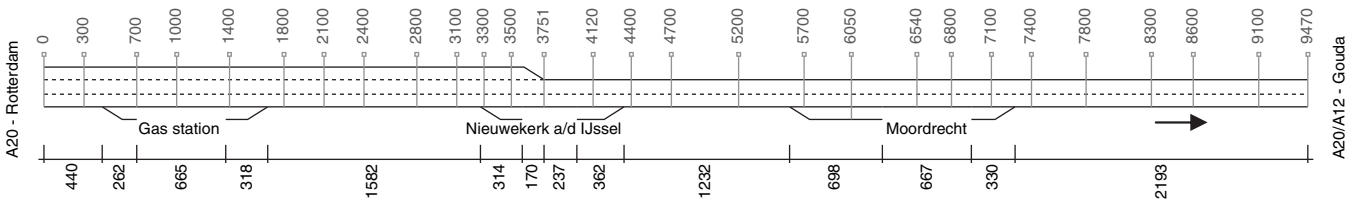

FIGURE 2 A20 network with distances and detector locations in meters.

1. For each parameter, look at two new points with a value that is a factor of $f(1)$ and $f(2)$ of the value in x.
   a. If a better point was found, set x at the best point. Redo Step 1.
   b. If no better point was found, go to Step 2.
2. Reduce the size of f by two-thirds; $f(2) = 1 + 2/3 \cdot (f(2) - 1)$ and $f(1) = 1/f(2)$.
   a. If $f(2) > 1.001$, redo Step 1.
   b. If $f(2) \leq 1.001$, stop.

To address the stochastic nature of the model, each error is an average error of five model runs with different random seeds. A higher number of runs would give more certainty but would also increase running times. Each simulation starts 10 min before the applicable period in order to fill the network.

Calibration and Validation Data

The model is calibrated with detector data on a section of the A20 freeway near Rotterdam, the Netherlands, as shown in Figure 2. The speed limit is 120 km/h. This section has a few on- and off-ramps and a lane drop and has closely spaced detectors (300 to 500 m). The data are too widely spaced for detection of actual lane changes. However, the main purpose of the model is to accurately represent lane distributions, lane specific speeds, and the onset and progression of congestion. These phenomena can be found in detector data, and the calibration is successful if these characteristics can be reproduced in simulation.

Congestion on the A20 toward Gouda is often initiated by spillback from the Moordrecht off-ramp. For calibration, the traffic state on the network must not be influenced by external phenomena, except for the demand pattern. A detector on the Moordrecht off-ramp (not shown in Figure 2) was used to find days in which congestion started due to the lane drop and Nieuwekerk aan den IJssel on-ramp and remained unaffected by the off-ramp for a considerable period. Two days were selected; Monday, June 8, 2009, and Thursday, June 25, 2009. The first day was used to calibrate free flow (5:15 to 6:15 a.m.) and congestion (6:00 to 7:00 a.m.), and the second day was used to validate free flow (5:30 to 6:30 a.m.) and congestion (6:15 to 7:15 a.m.). Truck percentages were very similar, at 11.0% and 10.6%, respectively.

Inflow into the model is based on detector data aggregated for 1 min. During each minute, the vehicles are uniformly distributed. The number of vehicles to be generated on the on-ramps was determined by subtracting the downstream flow from the upstream flow. This method may result in negative flows, solved by moving some vehicles earlier in time, which maintains the peaks in traffic demand.

Detector data were also used to estimate an origin–destination pattern, assuming a constant pattern over the simulated period. For each off-ramp, split fractions were determined. These were then used to assign probabilities of traffic from each origin toward the destinations, taking into account consecutive split fractions. Because the gas station is close to the beginning of the network, traffic toward the gas station is generated only on the right and middle lanes. Trucks are generated only on the right lane and on-ramps. Class-specific traffic counts on the A20 upstream of the network were used to estimate the percentage of trucks. These traffic counts were aggregated per month but separated per weekday.

Only detectors from $x = 1{,}400$ to $x = 7{,}400$ are considered for the error measure to allow traffic to settle and because speeds downstream of the Moordrecht on-ramp may be influenced by a narrow bridge and road curvature.

Results

Table 2 gives the calibrated parameter values. Some parameters have not changed or have changed little from the initial value. In general, these parameters have a range that may result in a more or less equal fit to data for as long as other parameters also change within such a range. Substantial changes from the initial values are found for a_{car}, b, σ_{car}, T_{min}, τ, t_0, and d_{free}. However, once these parameters receive a few course adjustments at the beginning of the calibration, a range of values again can result in a more or less equal fit.

A remarkable observation from the parameter values is that drivers apparently are willing to change lanes for a speed gain of $d_{free} \cdot v_{gain} \approx 25$ km/h or higher. This rather large value likely is not only a minimum speed gain but is simultaneously an adjustment of speed at both the origin and the target lane. For instance, a bounded driver on the right lane driving at 80 km/h who has a desired speed of 95 km/h is willing to overtake his leader by temporarily driving

TABLE 2 Calibration and Validation Errors

Day	Error Measure	Error Value
Free-Flow Scenario		
Monday, June 8, 2009 (calibration day)	RMSE flow (veh/h)	33.6
	RMSE speed (km/h)	4.70
	Total (ε_{free})	154.8
Thursday, June 25, 2009	RMSE flow (veh/h)	61.4
	RMSE speed (km/h)	5.35
	Total (ε_{free})	202.4
Congestion Scenario		
Monday, June 8, 2009 (calibration day)	RMSE flow (veh/h)	440
	RMSE speed (km/h)	22.6
	Total (ε_{cong})	1,011.6
Thursday, June 25, 2009	RMSE flow (veh/h)	373
	RMSE speed (km/h)	19.8
	Total (ε_{cong})	877.5

105 km/h in order not to hold up traffic on the left lane. The interpretation for v_{des} is thus a combination of desired speed and the speed at which drivers are willing to overtake. Such speed adaptation, however, is not explicitly modeled.

Another observation is that drivers look about 300 m (x_0) ahead on the right lane and will not keep right if there is a slower vehicle within this range. This may appear to be a rather long range; however, the value may result from the three-lane section, where traffic on the middle lane will not be inclined to keep right because they can still be overtaken. Also, some drivers may have little to no attention for the keep-right rule.

Figure 3 shows the calibrated lane fractions of the first run related to the density at a cross section with detectors. Lane fraction is the flow on a lane divided by the flow over all lanes. The density k_{road} is calculated as the flow over all lanes divided by the harmonic mean of the speeds on all lanes. The model represents the relationship between the density and the amount of traffic that can be found at different lanes. Furthermore, between $x = 2{,}400$ and $x = 3{,}500$, the amount of traffic on the left lane reduces as it will be dropped at $x = 3{,}751$. Consequently the amount of traffic on the middle lane increases, while the amount of traffic on the right lane changes little. At $x = 5{,}200$ there is more traffic on the right lane than at $x = 3{,}751$. This is because of the Moordrecht off-ramp, as well as traffic moving away from the busy left lane because of the upstream lane drop.

Calibrated speeds of the first run are shown at a three-lane cross section and a two-lane cross section. There are clear differences between lanes, and speeds appear to drop linearly for increasing density (in free flow). The model represents both phenomena. Runs 2 through 5 show results similar to Run 1 for lane fractions and lane speeds.

The results of the congestion scenario are presented in space–time–speed plots, which allow for good recognition of congestion patterns. These figures were created with the adaptive smoothing method (*24*). Figure 4 shows that the calibration runs can produce congestion comparable with reality. However, there are differences between congestion patterns, showing the influence of stochastic input. Similar plots were created for the validation day.

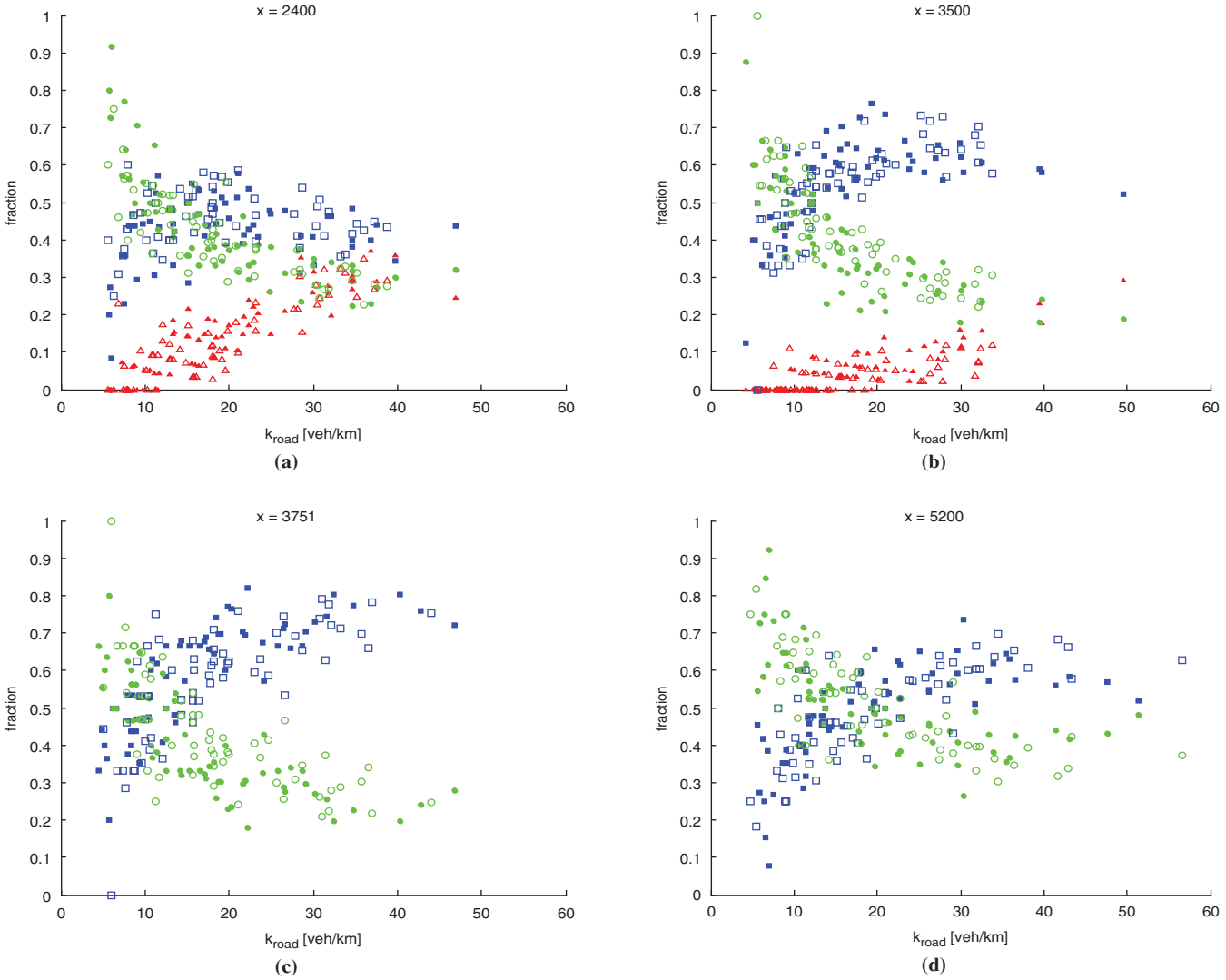

FIGURE 3 Calibrated lane fractions: (*a*) free flow (Run 1) at $x = 2{,}400$ m, (*b*) $x = 3{,}500$ m, (*c*) $x = 3{,}751$ m, and (*d*) $x = 5{,}200$ m.
(continued)

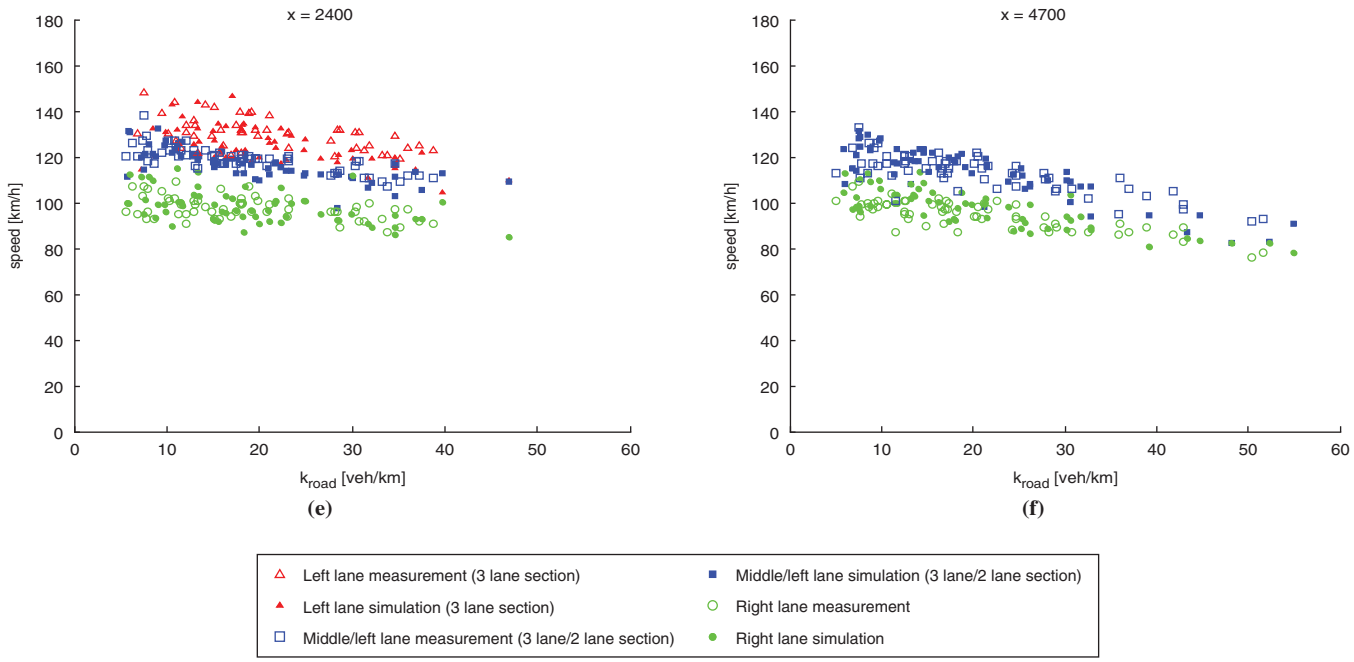

FIGURE 3 *(continued)* Calibrated lane speeds: (*e*) free flow (Run 1) at x = 2,400 m and (*f*) x = 4,700 m (each dot represents a 1-min measurement).

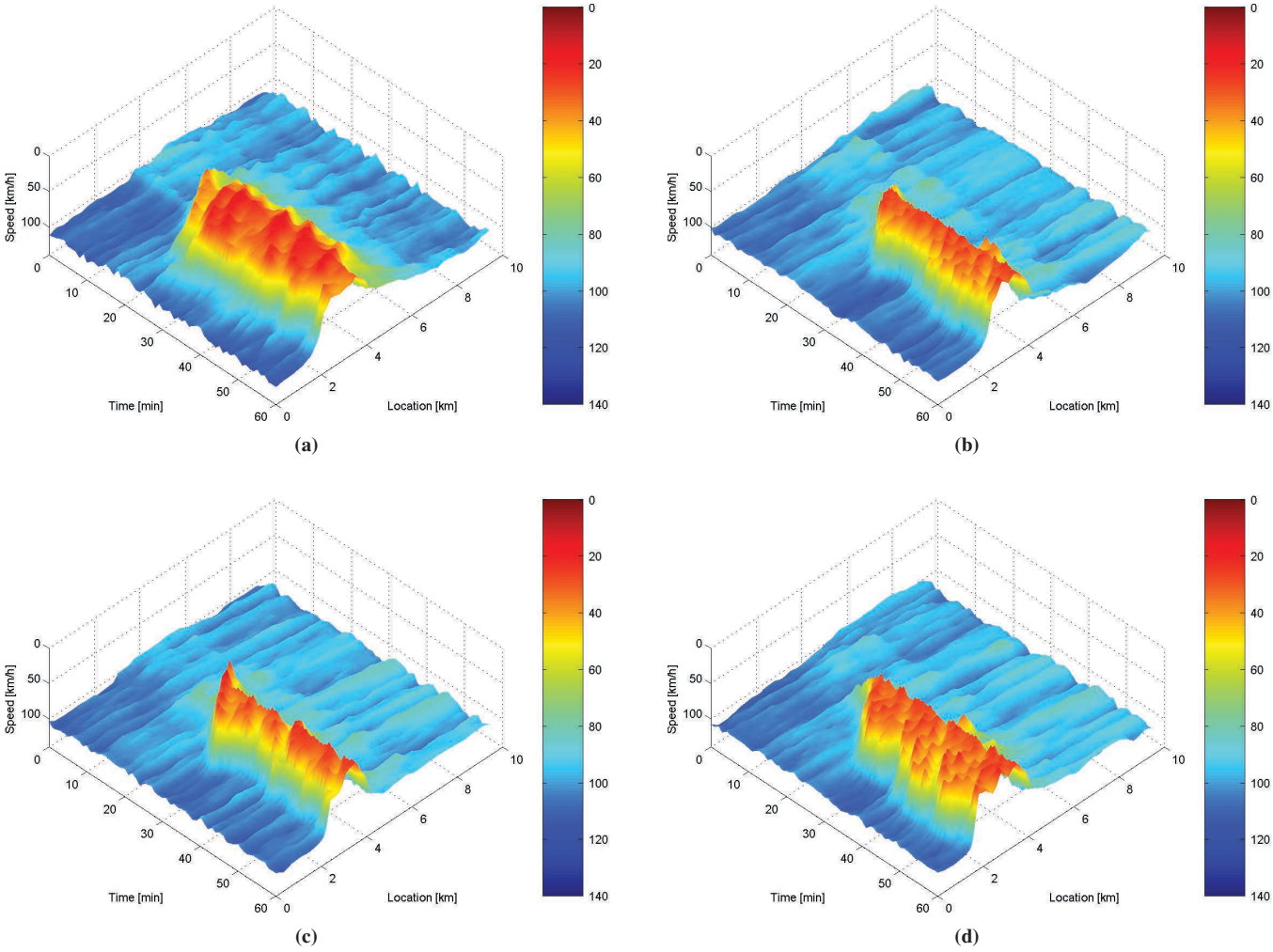

FIGURE 4 Speed pattern for calibration day June 8, 2009, in congestion scenario: (*a*) real data and (*b*) to (*d*) five model runs.

(continued on next page)

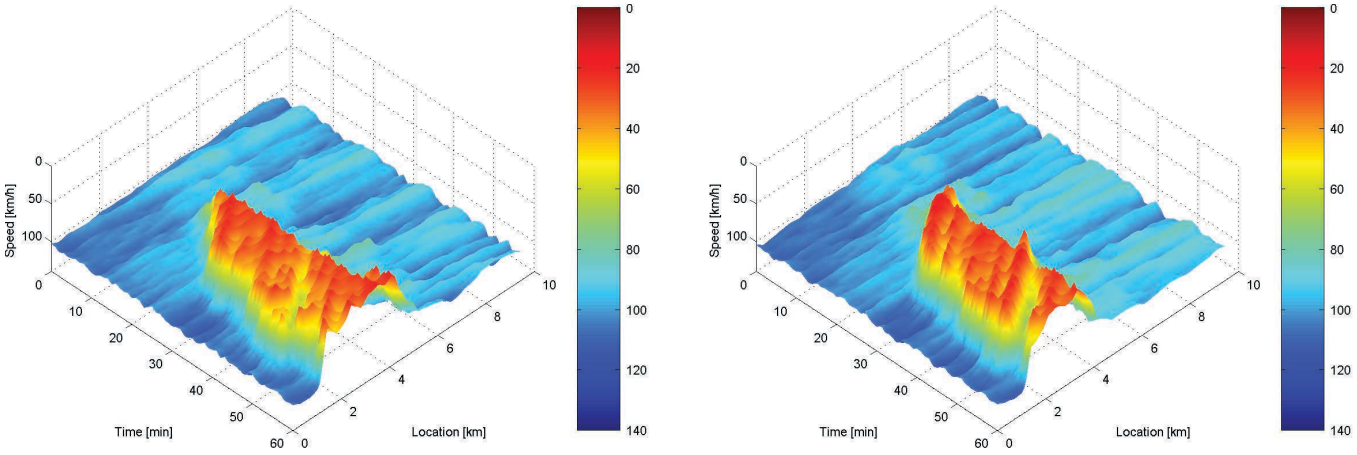

FIGURE 4 *(continued)* Speed pattern for calibration day June 8, 2009, in congestion scenario: (*e*) and (*f*) five model runs.

There was mild congestion in reality, but none of the five model runs showed congestion, although there were many drops in speed, none of which triggered congestion. These drops in speed indicate that congestion could arise with only small changes in input or parameter values.

Data from June 25, 2009 were used to validate the model. It is difficult to compare the model fit based on the error, because with more traffic the RMSE of flow will also increase for an equal error in terms of percentage. On June 25, there was 26% more traffic in the free-flow scenario, resulting in larger values of the RMSE of flow. This growth caused most of the increase of the total error in free flow. From this and the RMSE of speed, it can be concluded that the model does not appear to have a significantly different fit to data in free flow.

Traffic demand in the congestion scenario differs by only 1.2% between both days, but still the underlying demand pattern can strongly influence the amount of congestion. The error value is smaller on the validation day, although the fit appears worse than the calibration, as the validation runs produce no congestion. In general, the model shows a good fit to data. Validation results are reasonable given the large stochastic influence of driver behavior.

A sensitivity analysis was also performed to verify whether the calibration method using two scenarios was valid. Parameter values were changed from 50% to 150% of the original value while all other parameters remained fixed so changes in the error could be determined. It appeared that parameters were significant in their respective scenarios. More important, they were not significant in a wide range around their initial value in the scenario where they were kept constant.

SUMMARY AND CONCLUSIONS

A lane change model was proposed that is build around a lane change desire that follows from a combination of route, speed, and keep-right incentives. Within the combination of incentives there is a trade-off in which the route incentive becomes increasingly dominant. For an increasing level of lane change desire, drivers become more assertive. For little desire, no lane change will be performed. For slightly more desire, lane changes are performed only in a free fashion. For medium desire, drivers will start to synchronize with the target lane, and for high desire, the potential follower on the target lane is assumed to create a gap as it notices the lane change desire. The relaxation phenomenon is implemented as drivers accept smaller headways for larger desire.

The model was calibrated and validated in both free-flow and congested traffic conditions. Free flow gives a good fit to lane distributions for different levels of density on a particular cross section of the road. Speeds on the different lanes for different levels of density are also realistic. The fit in congestion is less clear because this depends highly on the stochastic input. For some runs, however, good fit was found on the location and moment of breakdown and the following progression of congestion. A sensitivity analysis showed that the two calibration scenarios are an appropriate approach.

The model can represent lane changing behavior with a set of seven parameters that all have physical and intuitive meaning. The model was calibrated and validated to a section on the A20 highway. Future research should investigate whether the model is applicable to other locations with different speed limits and more lanes. Also, the large speed threshold to change lanes indicates speed adaptation behavior. A more elaborate model regarding speed adaptation could improve results.

ACKNOWLEDGMENTS

This research was conducted as part of the Connected Cruise Control Project funded by the Dutch Ministry of Economic Affairs under the High Tech Automotive Systems Program by the Universities of Delft, Twente, and Eindhoven and by NXP, NAVTEQ, TNO, Clifford Electronics Benelux BV, Technolution, Rijkswaterstaat, and SWOV Institute for Road Safety Research.

REFERENCES

1. Gipps, P. G. A Behavioral Car Following Model for Computer Simulation. *Transportation Research Part B,* Vol. 15, No. 2, 1981, pp. 105–111.
2. Wiedemann, R. Simulation des Straßenverkehrsflusses. *Schriftenreihe des Institutes für Verkehrswesen der Universität Karlsruhe,* Vol. 8, 1974.

3. Bando, M., K. Hasebe, A. Nakayama, A. Shibata, and Y. Sugiyama. Dynamical Model of Traffic Congestion and Numerical Simulation. *Physical Review E,* Vol. 51, 1995, pp. 1035–1042.
4. Tampère, C. M. J. *Human-Kinetic Multiclass Traffic Flow Theory and Modeling*. PhD thesis. Delft University of Technology, Netherlands, 2004.
5. Treiber, M., A. Hennecke, and D. Helbing. Congested Traffic States in Empirical Observations and Microscopic Simulations. *Physical Review E,* Vol. 62, 2000, pp. 1805–1824.
6. Kesting, A., M. Treiber, and D. Helbing. General Lane-Changing Model MOBIL for Car-Following Models. In *Transportation Research Record: Journal of the Transportation Research Board, No. 1999,* Transportation Research Board of the National Academies, Washington, D.C., 2007, pp. 86–94.
7. Laval, J. A., and C. F. Daganzo. Lane Changing in Traffic Streams. *Transportation Research Part B,* Vol. 40, No. 3, 2006, pp. 251–265.
8. Gipps, P. G. A Model for the Structure of Lane Changing Decisions. *Transportation Research Part B,* Vol. 20, No. 5, 1986, pp. 403–414.
9. Toledo, T., H. N. Koutsopoulos, and M. Ben-Akiva. Integrated Driving Behavior Modeling. *Transportation Research Part C,* Vol. 15, No. 2, 2007, pp. 96–112.
10. Daamen, W., M. Loot, and S. P. Hoogendoorn. Empirical Analysis of Merging Behavior at Freeway On-Ramp. In *Transportation Research Record: Journal of the Transportation Research Board, No. 2188,* Transportation Research Board of the National Academies, Washington, D.C., 2010, pp. 108–118.
11. Laval, J. A., and L. Leclercq. Microscopic Modeling of the Relaxation Phenomenon Using a Macroscopic Lane Changing Model. *Transportation Research Part B,* Vol. 42, 2008, pp. 511–522.
12. Smith, S. A. *Freeway Data Collection for Studying Vehicle Interaction.* FHWA/RD-85/108. FHWA, U.S. Department of Transportation, 1985.
13. Sultan, B., M. Brackstone, B. Waterson, and E. R. Boer. Modeling the Dynamic Cut-In Situation. In *Transportation Research Record: Journal of the Transportation Research Board, No. 1803,* Transportation Research Board of the National Academies, Washington, D.C., 2002, pp. 45–51.
14. Wang, J., R. Liu, and F. Montgomery. A Simulation Model for Motorway Merging Behavior. *Proc., 16th International Symposium on Transportation and Traffic Theory* (H. S. Mahmassani, ed.), 2005, pp. 281–301.
15. Hidas, P. Modelling Lane Changing and Merging in Microscopic Traffic Simulation. *Transportation Research Part C,* Vol. 10, 2002, pp. 351–371.
16. Cohen, S. L. Application of Relaxation Procedure for Lane Changing in Microscopic Simulation Models. In *Transportation Research Record: Journal of the Transportation Research Board, No. 1883,* Transportation Research Board of the National Academies, Washington, D.C., 2004, pp. 50–58.
17. Yeo, H., A. Skabardonis, J. A. Halkias, J. Colyar, and V. Alexiadis. Oversaturated Freeway Flow Algorithm for Use in Next Generation Simulation. In *Transportation Research Record: Journal of the Transportation Research Board, No. 2088,* Transportation Research Board of the National Academies, Washington, D.C., 2008, pp. 68–79.
18. Choudhury, C. F., M. E. Ben-Akiva, T. Toledo, G. Lee, and A. Rao. Modeling Cooperative Lane Changing and Forced Merging Behavior. Presented at 86th Annual Meeting of the Transportation Research Board, 2007.
19. Dijker, T., and P. Knoppers. FOSIM 5.0 User Manual. 2004. www.fosim.nl.
20. Hoogendoorn, S. P., H. J. van Zuylen, M. Schreuder, B. Gorte, and G. Vosselman. Microscopic Traffic Data Collection by Remote Sensing. In *Transportation Research Record: Journal of the Transportation Research Board, No. 1855,* Transportation Research Board of the National Academies, Washington, D.C., 2003, pp. 121–128.
21. Daganzo, C. F. A Behavioral Theory of Multi-lane Traffic Flow. Part I: Long Homogeneous Freeway Sections. *Transportation Research Part B,* Vol. 36, No. 2, 2002, pp. 131–158.
22. Schakel, W. J., B. van Arem, and B. Netten. Effects of Cooperative Adaptive Cruise Control on Traffic Flow Stability. *Proc., 13th International IEEE Conference on Intelligent Transportation Systems,* 2010, pp. 759–764.
23. Ossen, S., and S. P. Hoogendoorn. Reliability of Parameter Values Estimated Using Trajectory Observations. In *Transportation Research Record: Journal of the Transportation Research Board, No. 2124,* Transportation Research Board of the National Academies, Washington, D.C., 2009, pp. 36–44.
24. Treiber, M., and D. Helbing. An Adaptive Smoothing Method for Traffic State Identification from Incomplete Information. In *Interface and Transport Dynamics: Computational Modelling* (H. Emmerich, B. Nestler, and M. Schreckenberg, eds.), Springer, Berlin, 2003, pp. 343–360.

The Traffic Flow Theory and Characteristics Committee peer-reviewed this paper, which was one of two papers that shared the 2012 Greenshields Prize awarded by the committee, honoring the contributions of Bruce Greenshields to the field of traffic flow theory.